



This discussion paper is/has been under review for the journal Atmospheric Chemistry and Physics (ACP). Please refer to the corresponding final paper in ACP if available.

A laboratory characterisation of inorganic iodine emissions from the sea surface: dependence on oceanic variables and parameterisation for global modelling

S. M. MacDonald¹, J. C. Gómez Martín¹, R. Chance², S. Warriner¹,
A. Saiz-Lopez³, L. J. Carpenter², and J. M. C. Plane¹

¹School of Chemistry, University of Leeds, Woodhouse Lane, Leeds, LS2 9JT, UK

²Department of Chemistry, University of York, Heslington, York, YO10 5DD, UK

³Atmospheric Chemistry and Climate Group, Institute of Physical Chemistry Rocasolano, CSIC, Madrid, Spain

Received: 30 October 2013 – Accepted: 25 November 2013 – Published: 2 December 2013

Correspondence to: J. M. C. Plane (j.m.c.plane@leeds.ac.uk)

Published by Copernicus Publications on behalf of the European Geosciences Union.

A laboratory characterisation of inorganic iodine emissions

S. M. MacDonald et al.

Title Page

Abstract

Introduction

Conclusions

References

Tables

Figures



Back

Close

Full Screen / Esc

Printer-friendly Version

Interactive Discussion

Abstract

Reactive iodine compounds play a significant role in the atmospheric chemistry of the oceanic boundary layer by influencing the oxidising capacity through catalytically removing O_3 and altering the HO_x and NO_x balance. The sea-to-air flux of iodine over the open ocean is therefore an important quantity in assessing these impacts on a global scale. This paper examines the effect of a number of relevant environmental parameters, including water temperature, salinity and organic compounds, on the magnitude of the HOI and I_2 fluxes produced from the uptake of O_3 and its reaction with iodide ions in aqueous solution. The results of these laboratory experiments and those reported previously (Carpenter et al., 2013), along with sea surface iodide concentrations measured or inferred from measurements of dissolved total iodine and iodate reported in the literature, were then used to produce parameterised expressions for the HOI and I_2 fluxes as a function of wind speed, sea-surface temperature and O_3 . These expressions were used in the Tropospheric HALogen chemistry MOdel (THAMO) to compare with MAX-DOAS measurements of iodine monoxide (IO) performed during the HaloCAST-P cruise in the Eastern Pacific ocean (Mahajan et al., 2012). The modelled IO agrees reasonably with the field observations, although significant discrepancies are found during a period of low wind speeds ($< 3 \text{ m s}^{-1}$), when the model overpredicts IO by up to a factor of three. The inorganic iodine flux contributions to IO are found to be comparable to, or even greater than, the contribution of organo-iodine compounds and therefore its inclusion in atmospheric models is important to improve predictions of the influence of halogen chemistry in the marine boundary layer.

1 Introduction

Reactive iodine compounds play an important role in the chemistry of the marine boundary layer (MBL) through their influence on ozone depletion and the oxidising capacity via repartitioning of HO_x and NO_x (Saiz-Lopez et al., 2012). Iodine oxides

ACPD

13, 31445–31477, 2013

A laboratory characterisation of inorganic iodine emissions

S. M. MacDonald et al.

Title Page

Abstract

Introduction

Conclusions

References

Tables

Figures

⏪

⏩

◀

▶

Back

Close

Full Screen / Esc

Printer-friendly Version

Interactive Discussion

A laboratory characterisation of inorganic iodine emissions

S. M. MacDonald et al.

Title Page

Abstract

Introduction

Conclusions

References

Tables

Figures

⏪

⏩

◀

▶

Back

Close

Full Screen / Esc

Printer-friendly Version

Interactive Discussion

also form new particles spontaneously in coastal (O'Dowd et al., 2002) and polar regions (Atkinson et al., 2012), potentially leading to the production of cloud condensation nuclei. In coastal regions, emissions of molecular iodine and to a lesser extent of halo-carbons from macroalgae are found to be the dominant source of reactive iodine to the MBL (O'Dowd et al., 2002). The source of reactive iodine and particles observed over the Antarctic sea ice remains to be determined (Atkinson et al., 2012).

Recent ground-, ship- and aircraft-based measurements have found that IO is ubiquitous over the open oceans, with MBL-averaged mixing ratios around 0.5 pptv, and surface mixing ratios of up to 3 pptv (Allan et al., 2000; Mahajan et al., 2010, 2012; Dix et al., 2013; Gómez Martín et al., 2013; Großmann et al., 2013). Modelling studies have shown that these levels of IO cannot be sustained by the measured iodocarbon fluxes and that an additional source of reactive iodine from the open ocean, equivalent to > 50 % of the total surface iodine emission, is required to match the observations. (Jones et al., 2010; Mahajan et al., 2010). Correlation studies of ground- and ship-based IO and reactive iodine ($IO_x = IO + I$) measurements with oceanic variables have shown that there is a negative correlation with Chla and CDOM, suggesting that the additional iodine production over the oceans is not biological and could be inhibited by the presence of increased biological activity or organic matter (Mahajan et al., 2012; Gómez Martín et al., 2013; Großmann et al., 2013). This provides evidence for the widespread abiotic iodine source proposed by Garland and Curtis (1981): the sea surface oxidation of I^- by O_3 to yield HOI and I_2 , which are then either released directly to the atmosphere or react with dissolved organic matter (Garland and Curtis, 1981; Martino et al., 2009; Carpenter et al., 2013). In addition, the correlation analysis showed significant correlations of IO_x with sea surface temperature (SST) and salinity (SSS), which suggests this abiotic mechanism will be influenced by oceanic variables.

Previously we provided the first experimental evidence that both I_2 and HOI are emitted from the reaction of $I^- + O_3$ in the interfacial layer, and that these emissions can account for the missing source of reactive iodine over the tropical Atlantic Ocean (Carpenter et al., 2013). In this paper we investigate the dependence of the flux of inorganic

iodine on relevant environmental parameters such as water temperature, salinity and the presence of organics. From these results and those previously reported (Carpenter et al., 2013), and using a kinetic model of the sea–air interface, parameterised expressions for the flux of both HOI and I₂ are derived. These expressions are then used in a 1-D atmospheric chemistry model for comparison with the field observations of reactive iodine species (IO and IO_x) recorded under a wide range of oceanic conditions during the HaloCAST-P cruise in the Eastern Pacific ocean (Mahajan et al., 2012).

2 Experimental

The experimental set-up used has been described in detail elsewhere (Carpenter et al., 2013, Supplement) and involves detection of I₂ and HOI released from an ozonised iodide solution through selective photolysis, reaction of the resulting I radicals with an excess of O₃ to form iodine oxide particles (IOPs) (Saunders et al., 2010), and subsequent detection of these particles using a nano-differential mobility analyser (nano-DMA) (Fig. 1). For the selective photolysis, two methods were used: a Xenon or Tungsten lamp along with suitable 10 nm bandwidth interference filters, or photolysis at either 532 nm (I₂) (Saiz-Lopez et al., 2004) or 355 nm (HOI) (Rowley et al., 1999) using a frequency doubled or tripled Nd:YAG laser (Continuum Surelite). The laser energy was continuously monitored using a powermeter (Molelectron Powermax 500A), so that the data could be normalised to the same pulse energy. The experimental setup was calibrated using a known flow of I₂ vapour, produced by passing N₂ over I₂ crystals (Sigma Aldrich), for each of the light sources used. A linear response over the range of I₂ concentrations observed in the experiments was found, giving a typical detection limit of around 2 pptv for I₂.

For the temperature dependence experiments a double-walled glass cell was used to allow cooled water to be flowed around the iodide solution. Temperatures ranging from 276 to 298 K were monitored using a thermocouple inserted into the solution in the cell. The iodide solutions were made up to the relevant concentrations using potassium io-

A laboratory characterisation of inorganic iodine emissions

S. M. MacDonald et al.

Title Page

Abstract

Introduction

Conclusions

References

Tables

Figures

⏪

⏩

◀

▶

Back

Close

Full Screen / Esc

Printer-friendly Version

Interactive Discussion

**A laboratory
characterisation of
inorganic iodine
emissions**

S. M. MacDonald et al.

Title Page

Abstract

Introduction

Conclusions

References

Tables

Figures

⏪

⏩

◀

▶

Back

Close

Full Screen / Esc

Printer-friendly Version

Interactive Discussion

dide (KI) (Alfa Aesar, A12704) dissolved in deionised water buffered to pH 8 using 0.1 M sodium phosphate (Sigma Aldrich). For the salinity dependence experiments, reagent grade NaCl (Fisher Scientific S/3160/53) was added to 1×10^{-6} M KI solutions to give concentrations ranging from 0 to 0.5 M Cl^- . To estimate the trace iodide present as a potential contaminant in the NaCl, 0.104 M solutions in water (LC-MS Chromasolv–Fluka 39253) containing variable concentrations of KI (concentrations ranging from 0 to 99.4×10^{-9} M, acquisitions performed in duplicate) were prepared and directly infused into a Bruker MaXis Impact Q-TOF mass spectrometer in negative electrospray ionisation mode. Full profile data were acquired with a 1 Hz acquisition rate for 3 min. The spectra were summed over the length of the acquisition and the relative intensity of the iodide peak (theoretical m/z 126.90522) relative to the cluster ion $(\text{NaCl})_2\text{Cl}^-$ (theoretical m/z 150.886645) was calculated. The spectra were calibrated using the $(\text{NaCl})_n\text{Cl}^-$ clusters as internal references. The observed mass of the iodide ion peak was within 3 ppm of the theoretical value in all cases.

For the experiments involving organics, in the case of humic acid (Sigma Aldrich) a small amount was added to a prepared iodide solution which was then stirred overnight and any remaining solid filtered off. The concentration of humic acid was determined by UV/Vis spectroscopy to be around 2 mg dm^{-3} . Sodium dodecyl sulphate (SDS, Sigma Aldrich) was added to a 1×10^{-7} M KI solution at a concentration of 6.2×10^{-3} M. Finally, for the experiments involving phenol, 1×10^{-7} M KI solutions containing phenol (Acros Organics) at concentrations ranging from 1×10^{-8} to 1×10^{-3} M were prepared.

3 Results

3.1 Salinity

The results of the salinity dependence experiments, using pH 8 buffered iodide solutions, are shown in Fig. 2. There is a clear increase in the I_2 flux with increasing salinity,

with the flux around 2.5 times higher at 0.5 M NaCl (roughly equivalent to a salinity of 32‰) compared to a solution containing no chloride.

The quantitative mass spectrometric analysis of the NaCl employed in these experiments allows us to rule out a significant contribution of an iodide impurity to the increasing I_2 flux. The relative intensity of the iodide mass peak observed in the 0.104 M NaCl solution was less than that observed in the sample spiked with 9.9×10^{-9} M KI. Therefore, the 0.5 M NaCl solution contained less than 50×10^{-9} M I^- impurity, a factor of 20 smaller than the 1×10^{-6} M I^- concentration employed in the salinity experiments.

3.2 Organics

A number of organic species were added to the KI aqueous solutions to investigate the effect of these compounds on the resulting I_2 flux. The first of these was humic acid (Sigma Aldrich), which was used as a proxy for dissolved organic matter found in seawater. Humic acid consists of a mixture of organic compounds formed from the degradation of organic matter. The I_2 flux was unaffected by the addition of relevant seawater concentrations ($\sim 2 \text{ mg dm}^{-3}$) of humic acid.

A further organic compound investigated was sodium dodecyl sulphate (SDS), which is a surfactant compound commonly found in a number of detergents and present at around $10 \mu\text{g dm}^{-3}$ in seawater (Ćosović et al., 1985). Surfactants are known to cause a reduction in the sea–air transfer of a number of atmospheric species by forming a barrier to emission. SDS was added to a 1×10^{-7} M KI solution at sufficient concentration to form a monolayer at the solution surface (6.2×10^{-3} M) (Hore et al., 2005). However, this amount of SDS was found to have no observable effect on the resulting IOP mass.

Previous studies have shown that phenol can have a significant effect on the I_2 flux in the $I^- + O_3$ reaction (Hayase et al., 2010). It is commonly found in seawater, mainly from anthropogenic sources at concentrations of around 1×10^{-8} to 1×10^{-7} M. In our experiments, using realistic seawater concentrations of both iodide (1×10^{-7} M) and phenol (1×10^{-8} – 1×10^{-7} M) there was no difference observed in the measured I_2 flux

A laboratory characterisation of inorganic iodine emissions

S. M. MacDonald et al.

Title Page

Abstract

Introduction

Conclusions

References

Tables

Figures

⏪

⏩

◀

▶

Back

Close

Full Screen / Esc

Printer-friendly Version

Interactive Discussion



within the 50 % uncertainty of the observed IOP mass. The phenol concentration had to be increased up to 1×10^{-3} M before a 50 % decrease in the I_2 flux was observed.

3.3 Temperature dependence

The temperature dependence of HOI and I_2 emissions from ozonised iodide solutions was investigated using both broadband light sources (xenon and tungsten lamps) and the Nd:YAG laser source to photolyse I_2 and HOI and produce detectable IOPs. The differing detection limits of the various systems necessitated different concentrations of I^- or O_3 to be able to measure both I_2 and HOI. The iodide concentration used in these experiments ranged from 1×10^{-6} – 5×10^{-6} M and the ozone ranged from 222–3600 ppbv. In order to account for changes in the observed I_2 and HOI fluxes caused by different ozone and iodide concentrations, as well as for pH variation with temperature, the HOI and I_2 fluxes were normalised by dividing through by the O_3 , I^- and H^+ concentrations according to the individual experiments (we have shown previously (Carpenter et al., 2013) that the HOI and I_2 fluxes are proportional to the concentrations of these species over the ranges employed here). The Arrhenius plots for the resulting normalised fluxes are shown in Fig. 3, along with the 95 % confidence limits for the activation energies. The resulting activation energy for the I_2 flux is $-7 \pm 18 \text{ kJ mol}^{-1}$, and $17 \pm 50 \text{ kJ mol}^{-1}$ for the HOI flux (at 95 % confidence). These large error bars result from poor reproducibility of the data, especially at low temperatures. This arose from the requirement to work at close to environmentally relevant concentrations of I^- and O_3 (within a factor of 10), in order to avoid non-linear effects in the HOI/ I_2 fluxes at higher concentrations. This resulted in a range of IOP numbers close to the detection limit of the particle counter, which reduced the precision of the measurements.

A laboratory characterisation of inorganic iodine emissions

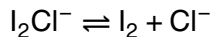
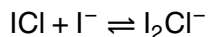
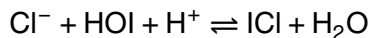
S. M. MacDonald et al.

[Title Page](#)[Abstract](#)[Introduction](#)[Conclusions](#)[References](#)[Tables](#)[Figures](#)[⏪](#)[⏩](#)[◀](#)[▶](#)[Back](#)[Close](#)[Full Screen / Esc](#)[Printer-friendly Version](#)[Interactive Discussion](#)

4 Discussion

4.1 Salinity

There do not appear to have been any previous studies investigating the effect of chloride concentration on the rate of the $\text{I}^- + \text{O}_3$ reaction. The kinetic interfacial model described in Carpenter et al. (2013) satisfactorily predicts the observed positive dependence of the I_2 flux on the Cl^- concentration (Fig. 2). The reason for this increase is due to conversion of a small amount of HOI into I_2 via ICl:



Note that this has very little effect on the HOI emission due to its great excess in the interfacial layer (Carpenter et al., 2013). As shown in Fig. 2, the observations exhibit a slightly larger chloride dependence, with a greater I_2 flux observed at 0.5 M Cl^- than the model predicts. This probably indicates the additional effect of the surface enhancement of I^- ions, which has been reported in a number of previous experimental and theoretical studies (Ghosal et al., 2005; Coleman et al., 2011; Gladich et al., 2011). In these studies I^- is shown to have a greater preference for the surface of an aqueous solution than Br^- or Cl^- , which has been explained by the more polarisable I^- anions having a lower excess surface free energy compared to either Br^- or Cl^- (Gladich et al., 2011).

Although there is a clear dependence of the I_2 flux on the Cl^- concentration, in seawater this effect is unlikely to be important due to the very small changes in SSS. Over the range of SSS commonly observed in the oceans (32–37‰), the resulting change in the I_2 flux based on the experimental results would be only around 1 %.

ACPD

13, 31445–31477, 2013

A laboratory characterisation of inorganic iodine emissions

S. M. MacDonald et al.

Title Page

Abstract

Introduction

Conclusions

References

Tables

Figures

⏪

⏩

◀

▶

Back

Close

Full Screen / Esc

Printer-friendly Version

Interactive Discussion

iodide solutions, under conditions of O_3 reactivity with iodide and DOC representative of the open ocean, which they have also attributed to a surface physical effect.

4.3 Temperature

Magi et al. (1997) used the droplet train technique to measure the disappearance of O_3 following uptake in I^- solution droplets (0.5–3 M NaI). The O_3 concentrations used were not stated in the paper. They reported a large positive temperature dependence for the $I^- + O_3$ rate coefficient, with an activation energy of $73 \pm 30 \text{ kJ mol}^{-1}$. However, the Arrhenius expression they reported ($k = 1.44 \times 10^{22} \exp(-73080/RT) \text{ M}^{-1} \text{ s}^{-1}$) contains a pre-exponential factor which is roughly 10 orders of magnitude greater than the diffusion limited reaction rate, and therefore appears to be unphysical.

Hu et al. (1995), using a similar droplet train technique with I^- concentrations from 0.5–3 M and O_3 in the range 5×10^{12} to $1 \times 10^{14} \text{ cm}^{-3}$, measured $k(I^- + O_3) = 4 \times 10^9 \text{ M}^{-1} \text{ s}^{-1}$ at 277 K. Although they do not report a room temperature measurement, the room temperature value for $k(I^- + O_3)$ appears to be reasonably well established from a number of previous studies (Garland et al., 1980; Hoigné et al., 1985; Magi et al., 1997; Liu et al., 2001), lying in the range $(1.2 - 2.4) \times 10^9 \text{ M}^{-1} \text{ s}^{-1}$. Thus the Hu et al. (1995) result implies a slightly negative temperature dependence, although those authors state that within their experimental accuracy the reaction could have been temperature independent.

We therefore assumed the temperature dependence for $k(I^- + O_3)$ to be zero for modelling the I_2 and HOI fluxes using the interfacial kinetic model (Carpenter et al., 2013). This gave an activation energy for the modelled I_2 emission between -6 and 2 kJ mol^{-1} over the concentration ranges of I^- and O_3 used in the present study, in agreement with the experimental results (Fig. 3). For HOI, the modelled activation energy ranged from 20 to 30 kJ mol^{-1} , again within experimental error (Fig. 3).

A laboratory characterisation of inorganic iodine emissions

S. M. MacDonald et al.

Title Page

Abstract

Introduction

Conclusions

References

Tables

Figures

⏪

⏩

◀

▶

Back

Close

Full Screen / Esc

Printer-friendly Version

Interactive Discussion

Truesdale et al., 2000; Huang et al., 2005) into an Arrhenius-type plot in Fig. 5. This exhibits a sensibly linear dependence of $\ln [I^-]$ with SST^{-1} (apart from a small number of outliers marked in red in Fig. 5). The resulting Arrhenius expression

$$[I_{(aq)}^-] = 1.46 \times 10^6 \times \exp\left(\frac{-9134}{SST}\right) \quad (1)$$

describes the iodide concentration (in mol dm^{-3}) at the sea surface as a function of SST (in K). From the 95 % prediction bands plotted in Fig. 5, the uncertainty in $[I^-]$ from Eq. (1) is estimated to be $\sim 50\%$ of the predicted value. This expression can then be incorporated into the flux expressions derived previously (Carpenter et al., 2013):

$$F_{\text{HOI}} = [O_{3(g)}] \times \left(4.15 \times 10^5 \times \left(\frac{\sqrt{[I_{(aq)}^-]}}{ws} \right) - \left(\frac{20.6}{ws} \right) - 23600 \times \sqrt{[I_{(aq)}^-]} \right) \quad (2)$$

$$F_{I_2} = [O_{3(g)}] \times [I_{(aq)}^-]^{1.3} \times (1.74 \times 10^9 - (6.54 \times 10^8 \times \ln ws)) \quad (3)$$

where the flux is in $\text{nmol m}^{-2} \text{d}^{-1}$, $[O_{3(g)}]$ is in ppbv (or nmol mol^{-1}), $[I_{(aq)}^-]$ in mol dm^{-3} and wind speed (ws) in m s^{-1} .

Equations (1)–(3) provide a more convenient parameterisation of the inorganic iodine flux for modelling purposes, since SST measurements are much more widely available than SSI measurements. Note that the fluxes are predicted to be highest under conditions of high $[O_{3(g)}]$, high $[I_{(aq)}^-]$, and/or low wind speed. The wind speed relationship arises from the assumption that wind shear (only) drives turbulent mixing of the interfacial layer with bulk seawater, thus reducing the proportion of I_2 and HOI evading into the atmosphere (Carpenter et al., 2013).

To test these expressions, daytime average measurements of IO_x recorded during the HaloCAST-P cruise in the eastern Pacific were compared with model output from the 1-D model THAMO (Saiz-Lopez et al., 2008). The HaloCAST-P cruise (Mahajan et al., 2012) was a 4-week cruise from 27 March to 26 April 2010, starting at

A laboratory characterisation of inorganic iodine emissions

S. M. MacDonald et al.

Title Page

Abstract

Introduction

Conclusions

References

Tables

Figures

◀

▶

◀

▶

Back

Close

Full Screen / Esc

Printer-friendly Version

Interactive Discussion



**A laboratory
characterisation of
inorganic iodine
emissions**

S. M. MacDonald et al.

Title Page

Abstract

Introduction

Conclusions

References

Tables

Figures

⏪

⏩

◀

▶

Back

Close

Full Screen / Esc

Printer-friendly Version

Interactive Discussion

Punta Arenas at the southern tip of Chile and continuing northwards to Seattle, USA. Measurements of IO were performed using a Multi-Axis Differential Optical Absorption Spectroscopy (MAX-DOAS) instrument, as well as measurements of CH_3I in seawater and air using gas chromatography-mass spectrometry (GC-MS) along with ancillary data such as SST, ws, Chl a , CDOM and SSS. IO_x mixing ratios were derived from the observed IO and CAM-Chem modelled O_3 , assuming low NO_x concentrations (O_3 was not measured during the cruise), for which the IO_x partitioning is controlled by IO photolysis and the $\text{I} + \text{O}_3$ reaction, resulting in an IO/I ratio of $\sim 0.12^* [\text{O}_3] \text{ ppbv}^{-1}$ (for $\text{SZA} < 60^\circ$).

Using the observed SST and ws from the HaloCAST-P cruise, and modelled O_3 from CAM-Chem (Fig. 6, Mahajan et al., 2012), the predicted HOI and I_2 fluxes were calculated using Eqs. (1)–(3). The sum of these is plotted against latitude in Fig. 6a and against the measured IO and derived IO_x in Fig. 7. The three points highlighted in red in Fig. 7 were excluded from the linear regression fits. These excluded points correspond to measurements at the equatorial front in the Pacific Ocean (15° – 25° N, see Fig. 6d), where the modelled O_3 concentrations are considerably more uncertain than earlier in the campaign. In this region the O_3 concentration is highly dependent on the water vapour concentration, which in turn will depend on the season and year due to fluctuations in temperature. As a result, the climatological O_3 output from CAM-Chem may not be representative of the actual O_3 during the Thompson cruise. The R^2 correlation coefficients with the IO_x and IO measurements (after excluding these points) were only 0.10 and 0.15 ($p = 0.09$), respectively. An interesting point to note is the significant intercept observed in both plots; 0.66 pptv for IO_x and 0.48 pptv for IO. This may be indicative of the contribution of iodocarbons to the total IO_x . The modelling work performed by Mahajan et al. (2012) suggested that around 30% of the IO_x could be explained by the observed emissions of CH_3I , and there are likely other iodocarbon species which will also contribute. As such, the 1-D model THAMO was initiated using only halocarbon fluxes with no contribution from the additional inorganic iodine emis-

sions so that the resulting IO and IO_x matched the observed intercepts. These values were then fixed for subsequent model runs.

THAMO is a 1-D chemistry transport model (Saiz-Lopez et al., 2008) consisting of 200 stacked boxes of 5 m resolution giving a total height of 1 km. K_{zz} profiles were constructed for each measurement point based on the measured ws, assuming convective conditions and a capped boundary layer of 1 km. A number of species were constrained in the model using typical measured values over the open ocean: [NO_x] = 25 pptv, [CO] = 110 ppbv, [DMS] = 30 pptv, [CH₄] = 1820 ppbv, [ethane] = 925 pptv, [CH₃CHO] = 970 pptv, [HCHO] = 500 pptv, [isoprene] = 10 pptv, [propane] = 60 pptv, [propene] = 20 pptv (Carpenter et al. (2013), Supplement). Equations (1)–(3) were included in THAMO to calculate the HOI and I₂ fluxes, driven by the measured ws and SST, and the CAM-Chem modelled O₃ mixing ratios at each point on the Thompson cruise track. Because HOI and I₂ can build up in the MBL close to the ocean surface, and therefore suppress the emission from the sea–air interface, the Henry’s law constants and transfer coefficients (K_T) for HOI and I₂ were calculated directly in the model (as described in Carpenter et al. (2013), Supplement).

The IO and IO_x predicted by THAMO, along with the measured IO and derived IO_x, were then plotted against latitude (Fig. 6d) and against the total inorganic iodine flux (Fig. 8). Note that the model IO and IO_x was computed by averaging over the first 200 m of the model vertical profiles (first 40 boxes) using only daylight data. This was done because the measured IO and IO_x mixing ratios were calculated from the MAX-DOAS IO slant column densities (dSCDs) measured with a 1° elevation angle, which should only be sensitive to the first 200 m in the boundary layer. The IO mixing ratios were then calculated using the O₄ method (Mahajan et al., 2012), and for quality control only daylight data with SZA < 60° were used.

Although there is reasonable agreement for the points with lower computed inorganic iodine flux, the predicted IO and IO_x is about a factor of 2 larger than measured at relatively high HOI and I₂ fluxes. Figure 6d also shows how the modelled IO_x around 20° N does not scale with the enhanced calculated flux at this latitude (equatorial front).

A laboratory characterisation of inorganic iodine emissions

S. M. MacDonald et al.

[Title Page](#)[Abstract](#)[Introduction](#)[Conclusions](#)[References](#)[Tables](#)[Figures](#)[⏪](#)[⏩](#)[◀](#)[▶](#)[Back](#)[Close](#)[Full Screen / Esc](#)[Printer-friendly Version](#)[Interactive Discussion](#)

$\sim 0.05 \text{ pptv K}^{-1}$, which compares well with the 0.03 pptv K^{-1} observed in the HaloCAST-P campaign.

Wind speed has a dramatic effect on the predicted IO and IO_x , with an increase observed at lower wind speeds. It is clear from inspection of Eq. 2 that the HOI flux will be heavily dependent on the wind speed due to the $w s^{-1}$ relationship. This means that Eq. 2 will become invalid at low wind speeds ($< 3 \text{ ms}^{-1}$). A comparison of the predicted HOI and I_2 fluxes using Eqs.(1)–(3) with the output of the kinetic interfacial model (Carpenter et al., 2013) shows that there is increasing deviation at wind speeds less than 3 ms^{-1} . For instance, Eqs.(1)–(3) overpredict the combined HOI and I_2 fluxes by a factor of two at a wind speed of 0.5 ms^{-1} .

4.6 Discussion of discrepancies between observed and predicted IO

The high predicted inorganic iodine flux around 20° N is generated by high O_3 (from CAM-Chem) and low measured wind speeds (see Fig. 6a, c and d). As mentioned above, the high O_3 from CAM-Chem may not accurately represent the O_3 during the Thompson cruise. In order to investigate this possibility, the model was run for the conditions of the three highest flux points in Fig. 8, varying the O_3 concentration until the resulting IO matched the measured mixing ratios (the IO was used to match the observations, as the IO_x measurements were derived from the O_3 mixing ratios predicted by CAM-Chem). The O_3 had to be reduced to 2 ppbv before the observations could be matched. In fact, open ocean ozone mixing ratios below the detection limit of commercial instruments ($\sim 2 \text{ ppbv}$) have been reported (Gómez Martín et al., 2013; Großmann et al., 2013). However, we have also shown above that an enhanced iodine inorganic flux due to high ozone mixing ratios does not result in a large increase of IO_x mixing ratios due the loss to IOPs via IO self reaction. This is clearly illustrated in Fig. 6 by similar modelled IO_x at 5° N and 20° N for similar wind speed and a difference of a factor of ~ 4 in the climatological ozone mixing ratios.

A laboratory characterisation of inorganic iodine emissions

S. M. MacDonald et al.

Title Page

Abstract

Introduction

Conclusions

References

Tables

Figures

⏪

⏩

◀

▶

Back

Close

Full Screen / Esc

Printer-friendly Version

Interactive Discussion

der real seawater conditions where the variations in salinity tend to be relatively small. None of the organics used in the reported experiments had any significant effect on the resulting inorganic iodine fluxes, but we cannot rule out the possibility that surface organic films may play a role in limiting the transfer of HOI and I₂ to the gas phase in real seawater.

SST was found to be a good proxy for SSI concentrations reported in the literature, and due to the wide availability of SST measurements, the derived relationship provides a useful tool for atmospheric modelling purposes. Modelled and measured IO and IO_x were found to be in reasonable agreement when the predicted I₂ and HOI fluxes were low, although under low wind speed conditions there is a substantial over-prediction in the model. A limiting factor may need to be introduced for modelling IO and IO_x under very calm ocean conditions. Based on the comparison with measurements in this paper, a simple approach would be to set a lower limit of ws to 3 ms⁻¹ when implementing Eqs.(1)–(3) in a model. The modelling results indicate that consideration of the inorganic iodine flux from reaction of O₃ and I⁻ is necessary for reproducing measurements of iodine oxides over the open ocean, although further experimental work is required to refine the parameterised flux expressions. These should be also tested against other long term/wide spatial coverage observations of reactive iodine recently reported.

References

Allan, B. J., McFiggans, G., Plane, J. M. C., and Coe, H.: Observations of iodine monoxide in the remote marine boundary layer, *J. Geophys. Res.-Atmos.*, 105, 14363–14369, doi:10.1029/1999jd901188, 2000.

Atkinson, H. M., Huang, R.-J., Chance, R., Roscoe, H. K., Hughes, C., Davison, B., Schönhardt, A., Mahajan, A. S., Saiz-Lopez, A., Hoffmann, T., and Liss, P. S.: Iodine emissions from the sea ice of the Weddell Sea, *Atmos. Chem. Phys.*, 12, 11229–11244, doi:10.5194/acp-12-11229-2012, 2012.

**A laboratory
characterisation of
inorganic iodine
emissions**

S. M. MacDonald et al.

Title Page

Abstract

Introduction

Conclusions

References

Tables

Figures

⏪

⏩

◀

▶

Back

Close

Full Screen / Esc

Printer-friendly Version

Interactive Discussion



- Caleman, C., Hub, J. S., van Maaren, P. J., and van der Spoel, D.: Atomistic simulation of ion solvation in water explains surface preference of halides, *P. Natl. Acad. Sci. USA*, 108, 6838–6842, doi:10.1073/pnas.1017903108, 2011.
- Carpenter, L. J., MacDonald, S. M., Shaw, M. D., Kumar, R., Saunders, R. W., Parthipan, R., Wilson, J., and Plane, J. M. C.: Atmospheric iodine levels influenced by sea surface emissions of inorganic iodine, *Nat. Geosci.*, 6, 108–111, doi:10.1038/ngeo1687, 2013.
- Ćosović, B., Žutić, V., Vojvodić, V., and Pleše, T.: Determination of surfactant activity and anionic detergents in seawater and sea surface microlayer in the Mediterranean, *Mar. Chem.*, 17, 127–139, doi:10.1016/0304-4203(85)90069-6, 1985.
- Dix, B., Baidar, S., Bresch, J. F., Hall, S. R., Schmidt, K. S., Wang, S., and Volkamer, R.: Detection of iodine monoxide in the tropical free troposphere, *P. Natl. Acad. Sci. USA*, 110, doi:10.1073/pnas.1212386110, 2013.
- Elderfield, H. and Truesdale, V. W.: On the biophilic nature of iodine in seawater, *Earth Planet. Sci. Lett.*, 50, 105–114, 1980.
- Frew, N. M., Bock, E. J., Schimpf, U., Hara, T., Haußecker, H., Edson, J. B., McGillis, W. R., Nelson, R. K., McKenna, S. P., Uz, B. M., and Jähne, B.: Air-sea gas transfer: its dependence on wind stress, small-scale roughness, and surface films, *J. Geophys. Res.-Oceans*, 109, C08S17, doi:10.1029/2003jc002131, 2004.
- Friedman, A. M. and Kennedy, J. W.: The self-diffusion coefficients of potassium, cesium, iodide and chloride ions in aqueous solutions, *J. Am. Chem. Soc.*, 77, 4499–4501, doi:10.1021/ja01622a016, 1955.
- Garland, J. A. and Curtis, H.: Emission of iodine from the sea-surface in the presence of ozone, *J. Geophys. Res.-Oceans*, 86, 3183–3186, 1981.
- Garland, J. A., Elzerman, A. W., and Penkett, S. A.: The mechanism for dry deposition of ozone to seawater surfaces, *J. Geophys. Res.-Ocean*, 85, 7488–7492, doi:10.1029/JC085iC12p07488, 1980.
- Ghosal, S., Hemminger, J. C., Bluhm, H., Mun, B. S., Hebenstreit, E. L. D., Ketteler, G., Ogletree, D. F., Requejo, F. G., and Salmeron, M.: Electron spectroscopy of aqueous solution interfaces reveals surface enhancement of halides, *Science*, 307, 563–566, doi:10.1126/science.1106525, 2005.
- Gladich, I., Shepson, P. B., Carignano, M. A., and Szleifer, I.: Halide affinity for the water-air interface in aqueous solutions of mixtures of sodium salts, *J. Phys. Chem. A*, 115, 5895–5899, doi:10.1021/jp110208a, 2011.

**A laboratory
characterisation of
inorganic iodine
emissions**

S. M. MacDonald et al.

Title Page

Abstract

Introduction

Conclusions

References

Tables

Figures

◀

▶

◀

▶

Back

Close

Full Screen / Esc

Printer-friendly Version

Interactive Discussion

- Gómez Martín, J. C., Mahajan, A. S., Hay, T. D., Prados-Román, C., Ordóñez, C., MacDonald, S. M., Plane, J. M. C., Sorribas, M., Gil, M., Paredes Mora, J. F., Agama Reyes, M. V., Oram, D. E., Leedham, E., and Saiz-Lopez, A.: Iodine chemistry in the eastern Pacific marine boundary layer, *J. Geophys. Res.-Atmos.*, 118, 887–904, doi:10.1002/jgrd.50132, 2013.
- 5 Großmann, K., Tschirter, J., Holla, R., Pöhler, D., Frieß, U., and Platt, U.: MAX-DOAS measurements of BrO and IO over the eastern Tropical North Atlantic, *Geophys. Res. Abstr.*, 13, EGU2011-8054-2011, 2011.
- Großmann, K., Frieß, U., Peters, E., Wittrock, F., Lampel, J., Yilmaz, S., Tschirter, J., Sommariva, R., von Glasow, R., Quack, B., Krüger, K., Pfeilsticker, K., and Platt, U.: Iodine monoxide in the Western Pacific marine boundary layer, *Atmos. Chem. Phys.*, 13, 3363–3378, doi:10.5194/acp-13-3363-2013, 2013.
- 10 Hayase, S., Yabushita, A., Kawasaki, M., Enami, S., Hoffmann, M. R., and Colussi, A. J.: Heterogeneous reaction of gaseous ozone with aqueous iodide in the presence of aqueous organic species, *J. Phys. Chem. A*, 114, 6016–6021, doi:10.1021/jp101985f, 2010.
- 15 Hayase, S., Yabushita, A., and Kawasaki, M.: Iodine emission in the presence of humic substances at the water's surface, *J. Phys. Chem. A*, 116, 5779–5783, doi:10.1021/jp2048234, 2012.
- Hoigné, J., Bader, H., Haag, W. R., and Staehelin, J.: Rate constants of reactions of ozone with organic and inorganic compounds in water – III. Inorganic compounds and radicals, *Water Res.*, 19, 993–1004, doi:10.1016/0043-1354(85)90368-9, 1985.
- 20 Hore, D. K., Beaman, D. K., and Richmond, G. L.: Surfactant headgroup orientation at the air/water interface, *J. Am. Chem. Soc.*, 127, 9356–9357, doi:10.1021/ja051492o, 2005.
- Hu, J. H., Shi, Q., Davidovits, P., Worsnop, D. R., Zahniser, M. S., and Kolb, C. E.: Reactive uptake of Cl_{2(g)} and Br_{2(g)} by aqueous surfaces as a function of Br- and I-ion concentration: the effect of chemical reaction at the interface, *J. Phys. Chem.*, 99, 8768–8776, doi:10.1021/j100021a050, 1995.
- 25 Huang, Z., Ito, K., Morita, I., Yokota, K., Fukushi, K., Timerbaev, A. R., Watanabe, S., and Hirokawa, T.: Sensitive monitoring of iodine species in sea water using capillary electrophoresis: vertical profiles of dissolved iodine in the Pacific Ocean, *J. Environ. Monit.*, 7, 804–808, doi:10.1039/b501398d, 2005.
- 30 Jones, C. E., Hornsby, K. E., Sommariva, R., Dunk, R. M., Von Glasow, R., McFiggans, G., and Carpenter, L. J.: Quantifying the contribution of marine organic gases to atmospheric iodine, *Geophys. Res. Lett.*, 37, L18804, doi:10.1029/2010gl043990, 2010.

A laboratory characterisation of inorganic iodine emissions

S. M. MacDonald et al.

Title Page

Abstract

Introduction

Conclusions

References

Tables

Figures

◀

▶

◀

▶

Back

Close

Full Screen / Esc

Printer-friendly Version

Interactive Discussion

- Liu, Q., Schurter, L. M., Muller, C. E., Aloisio, S., Francisco, J. S., and Margerum, D. W.: Kinetics and mechanisms of aqueous ozone reactions with bromide, sulfite, hydrogen sulfite, iodide, and nitrite ions, *Inorg. Chem.*, 40, 4436–4442, doi:10.1021/ic000919j, 2001.
- Magi, L., Schweitzer, F., Pallares, C., Cherif, S., Mirabel, P., and George, C.: Investigation of the uptake rate of ozone and methyl hydroperoxide by water surfaces, *J. Phys. Chem. A*, 101, 4943–4949, 1997.
- Mahajan, A. S., Plane, J. M. C., Oetjen, H., Mendes, L., Saunders, R. W., Saiz-Lopez, A., Jones, C. E., Carpenter, L. J., and McFiggans, G. B.: Measurement and modelling of tropospheric reactive halogen species over the tropical Atlantic Ocean, *Atmos. Chem. Phys.*, 10, 4611–4624, doi:10.5194/acp-10-4611-2010, 2010.
- Mahajan, A. S., Gómez Martín, J. C., Hay, T. D., Royer, S.-J., Yvon-Lewis, S., Liu, Y., Hu, L., Prados-Roman, C., Ordóñez, C., Plane, J. M. C., and Saiz-Lopez, A.: Latitudinal distribution of reactive iodine in the Eastern Pacific and its link to open ocean sources, *Atmos. Chem. Phys.*, 12, 11609–11617, doi:10.5194/acp-12-11609-2012, 2012.
- Martino, M., Mills, G. P., Woeltjen, J., and Liss, P. S.: A new source of volatile organoiodine compounds in surface seawater, *Geophys. Res. Lett.*, 36, L01609, doi:10.1029/2008gl036334, 2009.
- McTaggart, A. R., Butler, E. C. V., Haddad, P. R., and Middleton, J. H.: Iodide and iodate concentrations in eastern Australian subtropical waters, with iodide by ion chromatography, *Mar. Chem.*, 47, 159–172, doi:10.1016/0304-4203(94)90106-6, 1994.
- Nakayama, E., Kimoto, T., Isshiki, K., Sohrin, Y., and Okazaki, S.: Determination and distribution of iodide- and total-iodine in the North Pacific Ocean – by using a new automated electrochemical method, *Mar. Chem.*, 27, 105–116, doi:10.1016/0304-4203(89)90030-3, 1989.
- O'Dowd, C. D., Jimenez, J. L., Bahreini, R., Flagan, R. C., Seinfeld, J. H., Hameri, K., Pirjola, L., Kulmala, M., Jennings, S. G., and Hoffmann, T.: Marine aerosol formation from biogenic iodine emissions, *Nature*, 417, 632–636, 2002.
- Oetjen, H.: Measurements of Halogen Oxides by Scattered Sunlight Differential Optical Absorption Spectroscopy, Ph.D. thesis, Institut für Umweltp Physik, Bremen, Germany, Bremen, 2009.
- Read, K. A., Mahajan, A. S., Carpenter, L. J., Evans, M. J., Faria, B. V. E., Heard, D. E., Hopkins, J. R., Lee, J. D., Moller, S. J., Lewis, A. C., Mendes, L., McQuaid, J. B., Oetjen, H., Saiz-Lopez, A., Pilling, M. J., and Plane, J. M. C.: Extensive halogen-mediated ozone destruction over the tropical Atlantic Ocean, *Nature*, 453, 1232–1235, 2008.

**A laboratory
characterisation of
inorganic iodine
emissions**

S. M. MacDonald et al.

Title Page

Abstract

Introduction

Conclusions

References

Tables

Figures

◀

▶

◀

▶

Back

Close

Full Screen / Esc

Printer-friendly Version

Interactive Discussion

- Reeser, D. I. and Donaldson, D. J.: Influence of water surface properties on the heterogeneous reaction between $O_{3(g)}$ and $I_{-(aq)}$, *Atmos. Environ.*, 45, 6116–6120, 2011.
- Rouvière, A. and Ammann, M.: The effect of fatty acid surfactants on the uptake of ozone to aqueous halogenide particles, *Atmos. Chem. Phys.*, 10, 11489–11500, doi:10.5194/acp-10-11489-2010, 2010.
- Rowley, D., Mössinger, J., Cox, R. A., and Jones, R.: The UV-visible absorption cross-sections and atmospheric photolysis rate of HOI, *J. Atmos. Chem.*, 34, 137–151, doi:10.1023/a:1006210322389, 1999.
- Rutgersson, A., Smedman, A., and Sahlée, E.: Oceanic convective mixing and the impact on air–sea gas transfer velocity, *Geophys. Res. Lett.*, 38, L02602, doi:10.1029/2010gl045581, 2011.
- Saiz-Lopez, A. and Plane, J. M. C.: Novel iodine chemistry in the marine boundary layer, *Geophys. Res. Lett.*, 31, L04112, doi:10.1029/2003GL019215, 2004.
- Saiz-Lopez, A., Saunders, R. W., Joseph, D. M., Ashworth, S. H., and Plane, J. M. C.: Absolute absorption cross-section and photolysis rate of I_2 , *Atmos. Chem. Phys.*, 4, 1443–1450, doi:10.5194/acp-4-1443-2004, 2004.
- Saiz-Lopez, A., Plane, J. M. C., Mahajan, A. S., Anderson, P. S., Bauguitte, S. J.-B., Jones, A. E., Roscoe, H. K., Salmon, R. A., Bloss, W. J., Lee, J. D., and Heard, D. E.: On the vertical distribution of boundary layer halogens over coastal Antarctica: implications for O_3 , HO_x , NO_x and the Hg lifetime, *Atmos. Chem. Phys.*, 8, 887–900, doi:10.5194/acp-8-887-2008, 2008.
- Saiz-Lopez, A., Plane, J. M. C., Baker, A., Carpenter, L., von Glasow, R., Gómez Martín, J. C., McFiggans, G., and Saunders, R.: Atmospheric chemistry of iodine, *Chem. Rev.*, 112, 1773–1804, 2012.
- Saunders, R. W., Mahajan, A. S., Gómez Martín, J. C., Kumar, R., and Plane, J. M. C.: Studies of the Formation and Growth of Aerosol from Molecular Iodine Precursor, *Zeitschr. f. Phys. Chem. Munich*, 224, 1095–1117, 2010.
- Shaw, M. D. and Carpenter, L. J.: Modification of ozone deposition and I_2 emissions at the air–aqueous interface by dissolved organic carbon of marine origin, *Environ. Sci. Technol.*, 47, 10947–10954, 2013.
- Truesdale, V. W., Bale, A. J., and Woodward, E. M. S.: The meridional distribution of dissolved iodine in near-surface waters of the Atlantic Ocean, *Prog. Oceanograph.*, 45, 387–400, doi:10.1016/S0079-6611(00)00009-4, 2000.

Tsunogai, S. and Henmi, T.: Iodine in the surface water of the ocean, J. Oceanogr. Soc. Jpn., 27, 67–72, doi:10.1007/bf02109332, 1971.

5 Woittiez, J. R. W., van der Sloot, H. A., Wals, G. D., Nieuwendijk, B. J. T., and Zonderhuis, J.: The determination of iodide, iodate, total inorganic iodine and charcoal-adsorbable iodine in seawater, Mar. Chem., 34, 247–259, doi:10.1016/0304-4203(91)90006-I, 1991.

**A laboratory
characterisation of
inorganic iodine
emissions**

S. M. MacDonald et al.

Title Page

Abstract

Introduction

Conclusions

References

Tables

Figures

⏪

⏩

◀

▶

Back

Close

Full Screen / Esc

Printer-friendly Version

Interactive Discussion

A laboratory characterisation of inorganic iodine emissions

S. M. MacDonald et al.

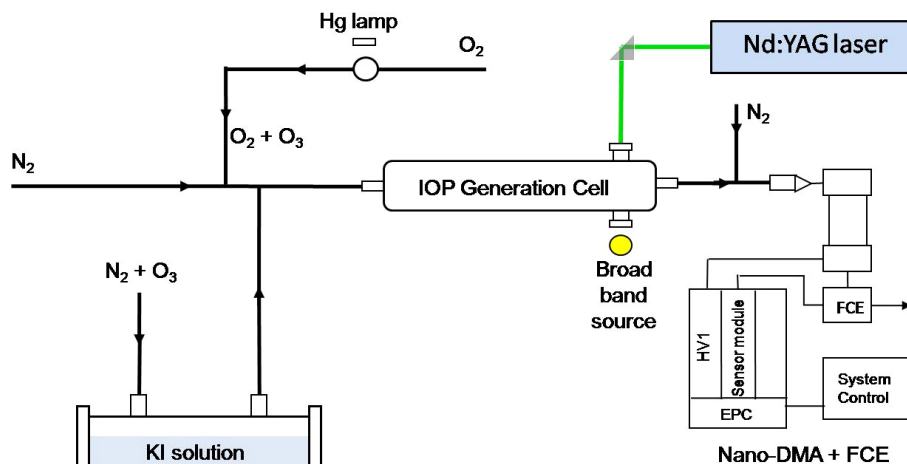


Fig. 1. Experimental setup showing the two different types of light sources (W/Xe lamp or Nd:YAG laser) used to photolyse and distinguish between I_2 and HOI.

A laboratory characterisation of inorganic iodine emissions

S. M. MacDonald et al.

Title Page

Abstract

Introduction

Conclusions

References

Tables

Figures

◀

▶

◀

▶

Back

Close

Full Screen / Esc

Printer-friendly Version

Interactive Discussion

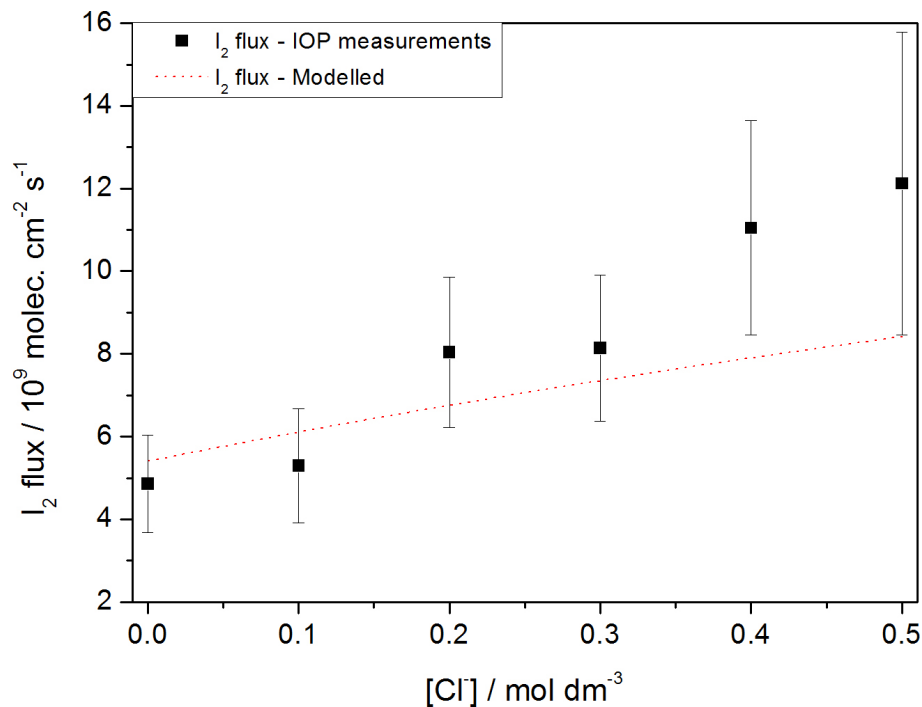


Fig. 2. I_2 flux from solution as a function of chloride concentration, showing a clear increase in both model (red dashed line) and measurements (black squares).

A laboratory characterisation of inorganic iodine emissions

S. M. MacDonald et al.

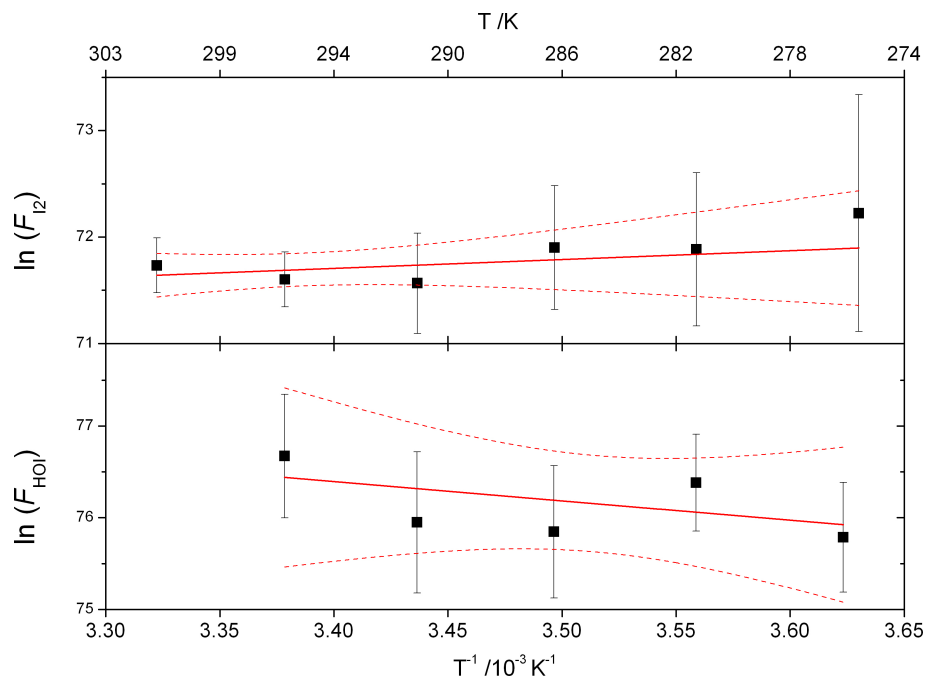


Fig. 3. Arrhenius plots for I₂ and HOI produced from the combined data using each light source normalised for [O₃], [I⁻] and [H⁺]. Dashed lines indicate the 95 % confidence limits of the linear fits.

A laboratory characterisation of inorganic iodine emissions

S. M. MacDonald et al.

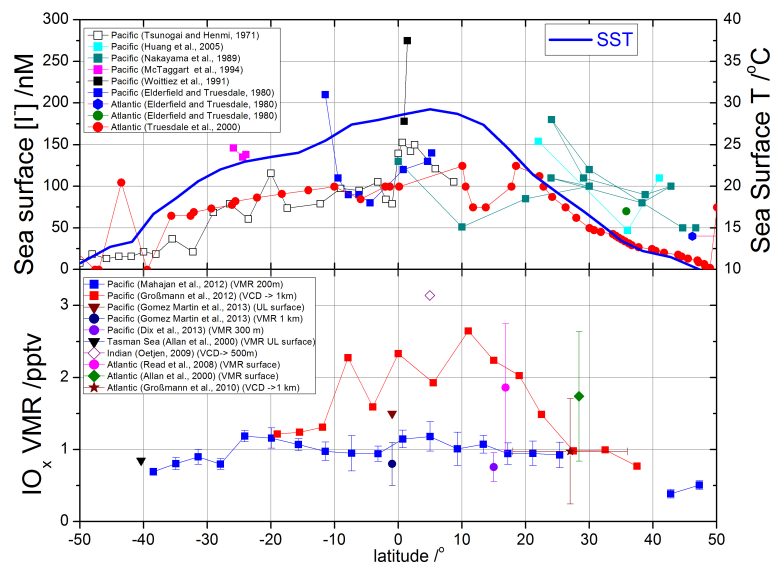


Fig. 4. The top panel shows measured sea surface iodide from a number of ship campaigns in the Pacific and Atlantic oceans (Tsunogai and Henmi, 1971; Elderfield and Truesdale, 1980; Nakayama et al., 1989; Woittiez et al., 1991; McTaggart et al., 1994; Truesdale et al., 2000; Huang et al., 2005) along with SST measurements in the Pacific Ocean in March–April 2010 (Mahajan et al., 2012). The bottom panel shows IO_x volume mixing ratios from campaigns in the open ocean at different latitudes (Allan et al., 2000; Read et al., 2008; Oetjen, 2009; Großmann et al., 2011, 2013; Mahajan et al., 2012; Dix et al., 2013; Gómez Martín et al., 2013). In the legend, VMR refers to volume mixing ratio (layer height stated for MAX-DOAS measurements), VCD refers to vertical column density converted to mixing ratio using the indicated column height, and UL means upper limit. Scaled VCDs are used instead of mixing ratios in some cases where the uncertainty range from radiative transfer calculations obscures the latitudinal variability.

Title Page

Abstract

Introduction

Conclusions

References

Tables

Figures

◀

▶

◀

▶

Back

Close

Full Screen / Esc

Printer-friendly Version

Interactive Discussion

A laboratory characterisation of inorganic iodine emissions

S. M. MacDonald et al.

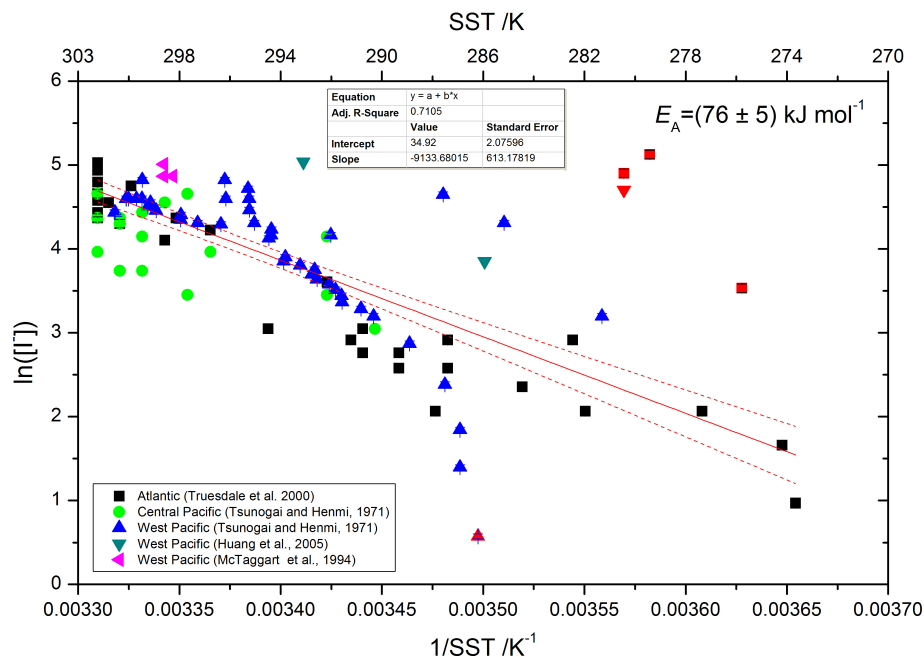


Fig. 5. Arrhenius plot of SSI vs. SST field measurements in the Pacific and Atlantic oceans (Tsunogai and Henmi, 1971; McTaggart et al., 1994; Truesdale et al., 2000; Huang et al., 2005). Red points are outliers removed from the fit (most of them correspond to a high iodide episode at low latitude during the Atlantic cruise). The activation energy obtained from the straight line fit is $(76 \pm 5) \text{ kJ mol}^{-1}$ ($R^2 = 0.71$). Dashed lines: confidence bands (red) at 95%.



Back

Close

Full Screen / Esc

Printer-friendly Version

Interactive Discussion



A laboratory characterisation of inorganic iodine emissions

S. M. MacDonald et al.

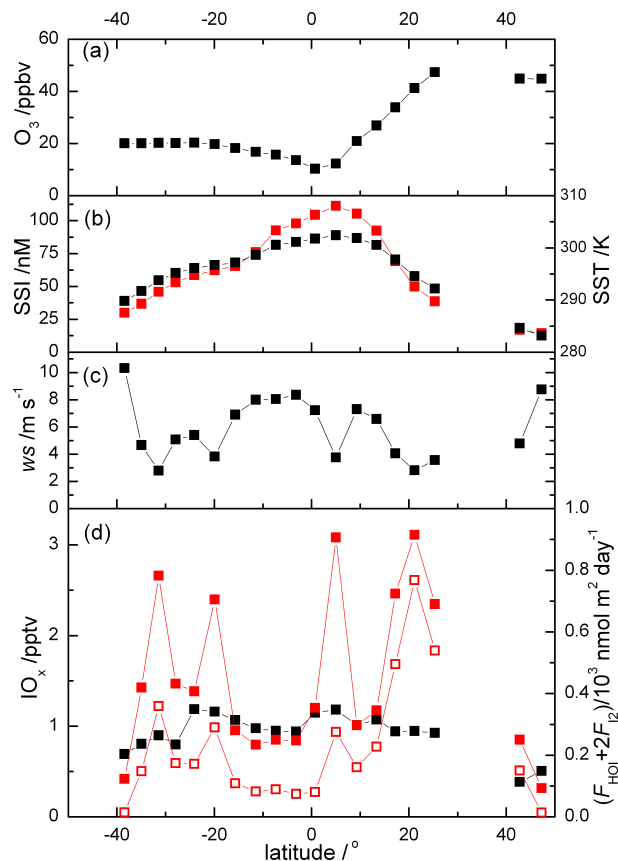


Fig. 6. HaloCAST-P cruise data (Mahajan et al., 2012): **(a)** ozone; **(b)** sea surface temperature (black, right axis) and iodide (red, left axis) derived from SST using Eq. (1); **(c)** wind speed; and **(d)** IO_x (left axis) and inorganic iodine flux (right axis). **(d)** Shows IO_x derived from measurements (black) and modelled in this work using THAMO (full red squares, left axis) employing the shown inorganic iodine source function (empty red squares, right axis).

A laboratory characterisation of inorganic iodine emissions

S. M. MacDonald et al.

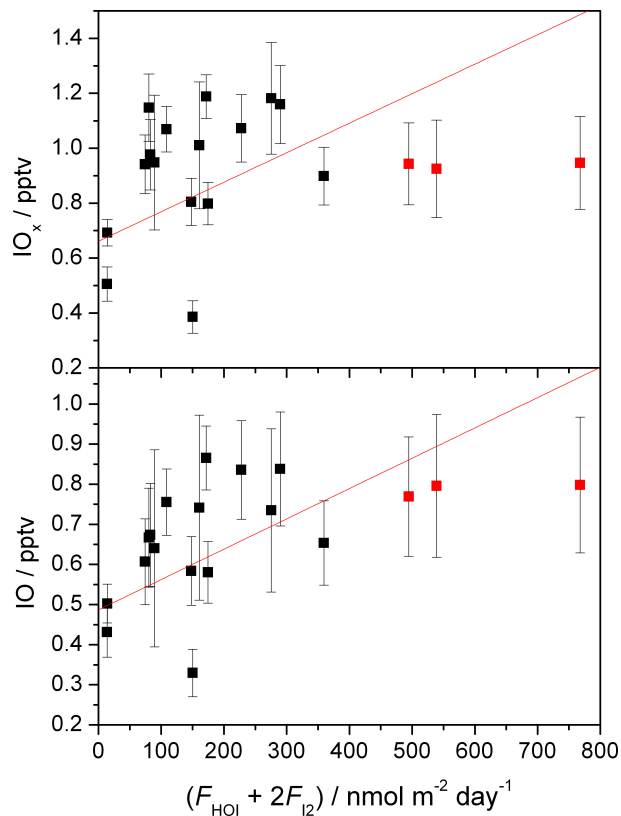


Fig. 7. Measured IO_x (top panel) and IO (bottom panel) from the HaloCAST-P cruise against predicted inorganic iodine flux from the parameterised flux expressions for each data point. Points in red were excluded from the linear fit.

[Title Page](#)[Abstract](#)[Introduction](#)[Conclusions](#)[References](#)[Tables](#)[Figures](#)[◀](#)[▶](#)[◀](#)[▶](#)[Back](#)[Close](#)[Full Screen / Esc](#)[Printer-friendly Version](#)[Interactive Discussion](#)

A laboratory characterisation of inorganic iodine emissions

S. M. MacDonald et al.

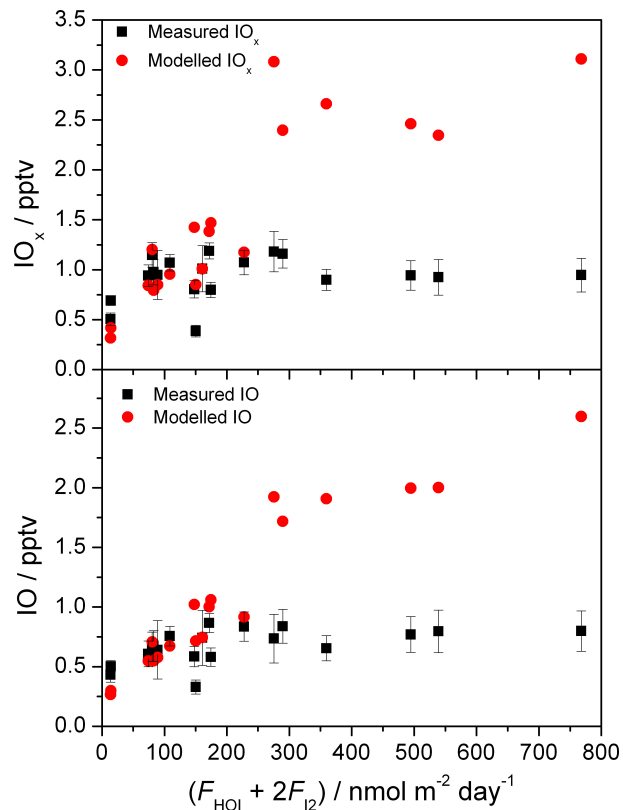


Fig. 8. Measured (black squares) and THAMO modelled (red circles) IO_x (top panel) and IO (bottom panel) for all HaloCAST-P cruise data against predicted inorganic iodine flux from the parameterised expressions.

[Title Page](#)[Abstract](#)[Introduction](#)[Conclusions](#)[References](#)[Tables](#)[Figures](#)[⏪](#)[⏩](#)[⏴](#)[⏵](#)[Back](#)[Close](#)[Full Screen / Esc](#)[Printer-friendly Version](#)[Interactive Discussion](#)

A laboratory characterisation of inorganic iodine emissions

S. M. MacDonald et al.

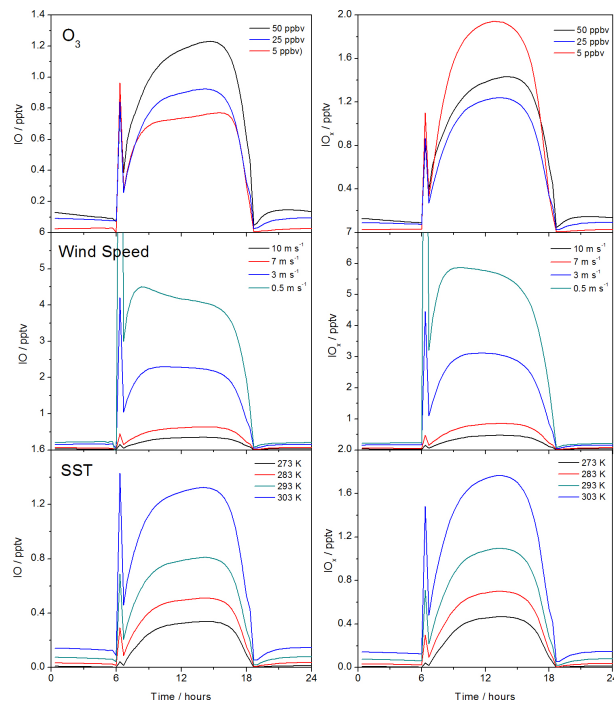


Fig. 9. Effect of changing flux parameters on the THAMO modelled mixing ratios of IO and IO_x averaged over the first 200 m. For each sensitivity test, the two fixed parameters are set to the average of the HaloCAST-P campaign: [O₃] = 25 ppbv, ws = 6 m s⁻¹ and SST = 296 K. Top panels: modelled diurnal IO and IO_x with varying O₃ (black line = 50 ppbv, blue line = 25 ppbv, red line = 5 ppbv). Middle panels: modelled diurnal IO and IO_x with varying wind speed (black line = 10 m s⁻¹, red line = 7 m s⁻¹, blue line = 3 m s⁻¹, turquoise line = 0.5 m s⁻¹). Bottom panels: modelled diurnal IO and IO_x with varying SST (black line = 273 K, red line = 283 K, turquoise line = 293 K, blue line = 303 K).

[Title Page](#)
[Abstract](#)
[Introduction](#)
[Conclusions](#)
[References](#)
[Tables](#)
[Figures](#)
[⏪](#)
[⏩](#)
[⏴](#)
[⏵](#)
[Back](#)
[Close](#)
[Full Screen / Esc](#)
[Printer-friendly Version](#)
[Interactive Discussion](#)